ELSEVIER

Neurocomputing 38–40 (2001) 159–166

NEUROCOMPUTING

www.elsevier.com/locate/neucom

A model of slow plateau-like oscillations based upon the fast Na^+ current in a window mode

G.S. Cymbalyuk*, R.L. Calabrese

Biology Department, Emory University, 1510 Clifton Road, Atlanta, GA 30322, USA

Abstract

Divalent ions, which block Ca^{2+} currents, combined with partial block of outward currents give rise to slow plateau-like oscillations (10–50 s period) with long duration plateaus and long inter-plateau intervals in leech heart interneurons (Opdyke, Calabrese, J. Comp. Physiol. 175 (1994) 781–789.) We present a simplified mathematical model that replicates the main characteristics of these observations and suggests an underlying biophysical mechanism. A model containing transient Na^+ current (I_{Na}), leakage and outward currents can generate oscillations with long plateau duration. The plateaus arise from a window mode of I_{Na} and do not require noninactivating Na^+ current (I_P). The long inter-plateau intervals are produced reliably after including I_P.

Keywords: Slow plateau-like oscillations; Window current; Sodium plateau

1. Introduction

Divalent ions like Co^{2+}, which block Ca^{2+} currents, cause slow oscillations of membrane potential in leech neurons [1]. Additionally, with partial block of outward currents, leech heart interneurons (HN) demonstrate slow plateau-like oscillations (8–60 s period) (Fig. 1) [13]. Blockade of hyperpolarization activated inward current by Cs^+ does not abolish the plateau-like oscillations, indicating that the presence of this current is not essential for the phenomenon [13].

These slow plateau-like oscillations pose two major challenges for mathematical modeling. What biophysical mechanisms give rise to (1) a long plateau duration (up to

* Corresponding author. Tel.: +1-404-727-4202; fax: +1-404-727-2880.
E-mail address: gcym@biology.emory.edu (G.S. Cymbalyuk).

0925-2312/01/$ - see front matter
PII: S0925-2312(01)00414-3

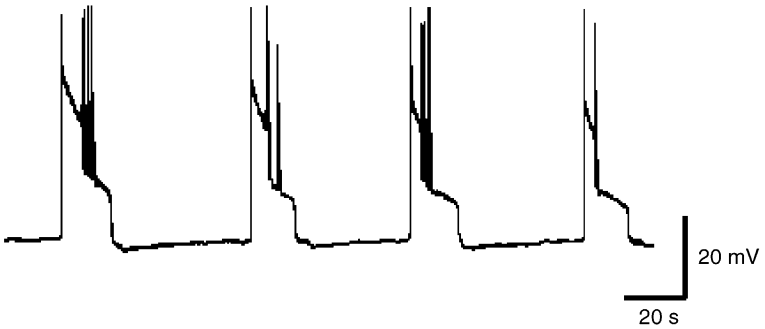

Fig. 1. Slow plateau-like oscillations occur in heart interneurons after bath application of Co^{2+} -containing saline and intracellular application of TEA^{+}.

20 s) and (2) a long inter-plateau interval (upto 40 s), when the time constants of currents involved do not exceed one second?

To explain these properties of the oscillations, [1] proposed a model based on an instantaneous, noninactivating Na^{+} current and a current produced by an electrogenic Na^{+}–K^{+} pump. The temporal characteristics of the oscillations were determined by the build up and the decay of the internal Na^{+} concentration, which activated and deactivated the pump.

Under similar experimental conditions, in other neurons, such as pyramidal cells of rat prefrontal cortex [16], Na^{+} plateaus can be activated with injected current. Dilmore et al. [5] investigated the plateau behavior of a model neuron with Na^{+} current dynamics including an additional slow inactivation variable. This model, which introduced two different time scales for the Na^{+} current, is sufficient to explain plateau potentials [6]. Our previous paper [4] showed that the Dilmore model is not a minimal model for the plateau behavior, because a model containing the fast Na^{+} current without a slow component is sufficient. The plateau in our model is due to the effect of a window mode of I_{Na}. The window mode of a fast current produces a steady current as a result of the overlap between the steady state activation and inactivation curves. This overlap defines the window, i.e. the range of voltages where substantial steady current exists.

Our full model of an HN neuron includes 9 observed currents [11,12,7]. Here we investigate a simplified model of an HN neuron to define biophysical mechanisms that could account for the properties of very slow plateau-like oscillations. The contribution of I_{Na} is most directly illustrated by a minimal model containing three currents, I_{Na}, I_l, and I_{K2} [4]. The study of this model suggests that plateau behavior is supported by a window mode of I_{Na}. To achieve a sufficiently long inter-plateau interval during oscillation we added I_P.

2. Methods

Here we employ three simplified models, each described by different number of differential equations. In the text, we refer to these models by corresponding roman

numerals (II, IV and V). Model IV contains a fast Na^+ current (I_{Na}), a persistent K^+ current (I_{K2}), and a leakage current (I_l) and is described by 4 stiff differential equations (Appendix A). To qualitatively explain how plateau-like oscillations appear in this system we dissect model IV, reducing it to a second order system. This reduction takes into account that the activation of $I_{Na}(m_{Na})$ is the "fastest" variable and activation of $I_{K2}(m_{K2})$ is the slowest variable (see also [10,15,3,8]). Model II is described by the membrane potential (V) and the inactivation of $I_{Na}(h_{Na})$. Using m_{K2} as a parameter we calculate the bifurcation diagram of stationary states and limit cycles of model II (Fig. 2).

Finally, we show that when model IV is augmented by the incorporation of I_P (model V), it can achieve long inter-plateau intervals. Also, the set of currents of model V conforms to the experimental conditions described above, i.e. Ca^{2+}, K^+ and hyperpolarization activated inward current are blocked pharmacologically.

Integration of equations and bifurcation analysis were carried out by using LocBif [9] http://locbif.tripod.com) and XPPAUTO (developed by G.B. Ermentrout and available at ftp://ftp.math.pitt.edu/pub/bardware/).

3. Results

The basic biophysical mechanism underlying the slow plateau-like oscillations is illustrated in Fig. 2. The bifurcation diagram of model II presents a knee shaped curve of stationary points for different values of m_{K2}. The top branch represents depolarized stationary points. Up to $m_{K2} = B$ it depicts the dependence of the depolarized rest potential on m_{K2}; for $m_{K2} > B$ it depicts unstable depolarized stationary points which end at the knee. The bottom branch represents stable hyperpolarized stationary points and, correspondingly, depicts the dependence of the hyperpolarized rest potential on m_{K2}. These branches are connected by the curve representing unstable stationary points of a saddle type. At $m_{K2} = A$ the saddle point and stable hyperpolarized stationary point coalesce at a saddle-node bifurcation. At point B the depolarized stationary state becomes unstable and gives rise to a stable limit cycle via a supercritical Andronov–Hopf bifurcation. At $m_{K2} = C$ an unstable limit cycle appears via a saddle homoclinic bifurcation. At $m_{K2} = D$, both limit cycles disappear on a fold bifurcation for limit cycles (points C and D are located near each other and are lumped together in Fig. 2). Thus, for values of m_{K2} below A, there is only one stationary state, defined by the depolarized rest potential. This means that starting from any initial conditions model II ends at the depolarized rest potential. For m_{K2} taken between A and B there are two stable stationary states, one with the depolarized rest potential and one with the hyperpolarized rest potential. Depending on the initial conditions, model II ends up at one of them. For m_{K2} taken between B and D there are two stable regimes, one is the hyperpolarized stationary state and the other is the stable limit cycle. Within this range, the amplitude of the stable limit cycle grows monotonically as m_{K2} increases. For m_{K2} larger than D there is again only one stationary state, defined by the hyperpolarized rest potential.

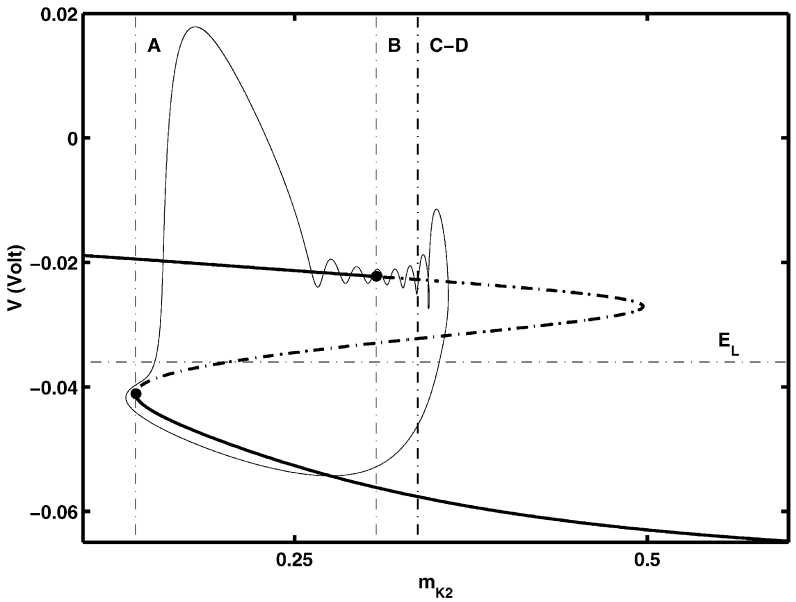

Fig. 2. Bifurcation diagram of the reduced system (model II). Solid thick curve represents stable stationary points, dashed thick curve represents unstable stationary points when m_{K2} is varied. Closed orbit (solid thin curve) is the projection of the stable limit cycle of the minimal model (model IV) onto the (V, m_{K2}) plane of bifurcation diagram. Vertical dashed lines mark A, B, C, D points which correspond to saddle-node, supercritical Andronov–Hopf, saddle homoclinic bifurcations and fold bifurcation for limit cycles, respectively. Values of m_{K2} for bifurcation points are A = 0.13747, B = 0.30791, C = 0.33696, D = 0.33764.

Let us consider a projection of plateau-like oscillations observed in model IV on the (V, m_{K2}) plane of the bifurcation diagram. The plateau phase starts with a large amplitude spike. Then, the potential decays to a plateau supported by a window mode of I_{Na} and oscillates around the depolarized rest potential of model II. During this phase, m_{K2} slowly grows. Note that the amplitude of model IV oscillations decreases when m_{K2} approaches B and increases after m_{K2} passes B. This observation is a manifestation of the transition of model II from the stable stationary state to the stable limit cycle when m_{K2} crosses B. In model IV, soon after m_{K2} passes point D, the membrane potential quickly decreases towards the hyperpolarized stationary state of model II (Fig. 2). The duration of the plateau is mainly determined by the size of the imbalance between the I_{Na} window current, and I_{K2} and I_1.

I_{K2} slowly deactivates during the inter-plateau phase. During this phase the membrane potential follows the hyperpolarized rest potential of model II. In model IV, I_{Na} activates because the membrane potential approaches E_L, which was made significantly more depolarized ($E_l = -0.036$ V) than has been experimentally observed ($E_l \approx -0.055$). Once I_{Na} activates, the plateau phase begins again when m_{K2} is close to A with a large amplitude spike (Fig. 3).

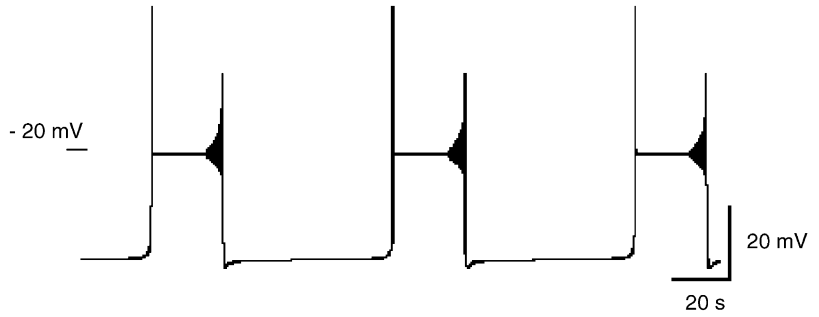

Fig. 3. Slow plateau-like oscillations in model V based on dynamics of the currents—I_{Na}, I_P, I_{K2}, and I_l.

The model IV can produce oscillations with long duration plateaus (Fig. 3). However, according to our observations, it fails to explain the long inter-plateau intervals observed in the biological system. Augmentation of model IV by the introduction of I_P allowed us to match the long inter-plateau intervals. The inter-plateau interval is mainly determined by the size of the imbalance between I_P and I_l, and I_{K2}. The advantage of model V over model IV is based upon the notion that at hyperpolarized potentials I_P and I_{K2} operate on similar time scales. This makes it easier to bring them into balance and, thus, obtain long inter-plateau intervals. Note that in this model I_P depolarizes the membrane potential causing activation of I_{Na}. Thus, E_l now conforms to experimentally measured values ($E_l = -0.058$ V).

4. Conclusions

The experiments in which Ca^{2+} currents are blocked and outward currents are reduced provide additional constraints for mathematical modeling and leads to a better understanding of the biophysical mechanisms governing neuronal behavior. The described biophysical mechanisms can account for the properties of slow plateau-like oscillations observed in HN cells under these conditions.

We show that the classical presentation of the transient Na^+ current is sufficient for the production of plateau behavior due to properties of the window current. The simplified model (II) can provide slow plateau-like oscillations with a sufficiently long plateau phase. A noninactivating Na^+ current is exploited here to explain long inter-plateau intervals.

According to a classification of bursting oscillations based on a singular perturbation analysis, also called a dissection technique, the generation of slow plateau-like oscillations is similar to the generation of square-wave bursts [2,8,14]. The main difference is that in our reduced model fast oscillations disappear via a fold bifurcation, whereas in a reduced model of square-wave bursting they disappear via a saddle homoclinic bifurcation. Also, in our model the fast oscillations appear via a supercritical Andronov–Hopf bifurcation, explaining the existence of the plateaus, whereas in the square-wave bursting model they appear via a subcritical Andronov–Hopf bifurcation.

We have outlined potential biophysical mechanisms involved in the generation of slow plateau-like oscillations. In future we plan to analyze in more detail the minimal model (model IV) and its reduction (model II) under different parameter regimes and to compare them to a similar analysis of the minimal model incorporating I_P (model V). We expect that this analysis will contrast the roles of I_{Na} and I_P in generating the slow plateau-like oscillations.

Acknowledgements

We are grateful to Andrew Hill and Mark Masino for careful reading of the manuscript. This work was supported by NIH grants NS24072.

Appendix A

The dynamics of the single neuron is described by the single compartment model complying with Hodgkin–Huxley formalism. The parameter values are presented in the captions to the figures.

Model II:

$$C\frac{dV}{dt} = -(\bar{g}_{Na}m_{Na}^3h_{Na}(V-E_{Na}) + \bar{g}_{K2}m_{K2}^2(V-E_K) + \bar{g}_l(V-E_l)),$$

$$\frac{dh_{Na}}{dt} = \frac{f_\infty(500, 0.027, V) - h_{Na}}{\tau_{h_{Na}}(V)},$$

where $m_{Na} = f_\infty(-150, 0.027, V)$, $C = 0.5\,pF$, $E_{Na} = 0.045\,V$, $E_K = -0.07\,V$, $E_l = -0.036\,V$, $\bar{g}_{Na} = 200\,nS$, $\bar{g}_{K2} = 80\,nS$, $\bar{g}_1 = 6.5\,nS$ and m_{Na} is used as a bifurcation parameter.

Model IV:

$$C\frac{dV}{dt} = -(\bar{g}_{Na}m_{Na}^3h_{Na}(V-E_{Na}) + \bar{g}_{K2}m_{K2}^2(V-E_K) + \bar{g}_1(V-E_l)),$$

$$\frac{dm_{Na}}{dt} = \frac{f_\infty(-150, 0.027, V) - m_{Na}}{0.0001},$$

$$\frac{dh_{Na}}{dt} = \frac{f_\infty(500, 0.027, V) - h_{Na}}{\tau_{h_{Na}}(V)},$$

$$\frac{dm_{k2}}{dt} = \frac{f_\infty(-80, 0.018, V) - m_{K2}}{0.25},$$

where $C = 0.5\,pF$, $E_{Na} = 0.045\,V$, $E_K = -0.07\,V$, $E_l = -0.036\,V$, $\bar{g}_{Na} = 200\,nS$, $\bar{g}_{K2} = 80\,nS$, $\bar{g}_1 = 6.5\,nS$.

Model V:

$$C\frac{dV}{dt} = -(\bar{g}_{Na}m_{Na}^3 h_{Na}(V - E_{Na}) + \bar{g}_{K2}m_{K2}^2(V - E_K) + \bar{g}_P m_P(V - E_{Na}) + \bar{g}_l(V - E_l)),$$

$$\frac{dm_{Na}}{dt} = \frac{f_\infty(-150, 0.027, V) - m_{Na}}{0.0001},$$

$$\frac{dh_{Na}}{dt} = \frac{f_\infty(500, 0.026, V) - h_{Na}}{\tau_{h_{Na}}(V)},$$

$$\frac{dm_P}{dt} = \frac{f_\infty(-120, 0.039, V) - m_P}{\tau(400, 0.057, 0.01, 0.2, V)}m,$$

$$\frac{dm_{k2}}{dt} = \frac{f_\infty(-80, 0.018, V) - m_{K2}}{0.25},$$

where $C = 0.5\,\text{pF}$, $E_{Na} = 0.045\,\text{V}$, $E_k = -0.07\,\text{V}$, $E_l = -0.058\,\text{V}$, $\bar{g}_{Na} = 200\,\text{nS}$, $\bar{g}_P = 6.156\,\text{nS}$, $\bar{g}_{K2} = 97.1\,\text{nS}$, $\bar{g}_l = 6.5\,\text{nS}$.

Functions used in the equations are

$$f_\infty(a, b, V) = 1/1 + e^{a(V+b)},$$

$$\tau(a, b, c, d, V) = c + \frac{d}{1 + e^{a(V+b)}},$$

$$\tau_{mCaF}(V) = 0.011 + \frac{0.024}{\cosh(-330(V + 0.0467))}$$

$$\tau_{h_{Na}}(V) = 0.004 + \frac{0.006}{1 + e^{500(V+0.028)}} + \frac{0.01}{\cosh(300(V + 0.027))}.$$

References

[1] J.D. Angstadt, W.O. Friesen, Synchronized oscillatory activity in leech neurons induced by calcium channel blockers, J. Neurophysiol. 66 (1991) 1858–1873.

[2] R. Bertram, M.J. Butte, T. Kiemel, A. Sherman, Topological and phenomenological classification of bursting oscillations, Bull. Math. Biol. 57 (1995) 413–439.

[3] R.J. Butera, J.W. Clark, J.H. Byrne, Dissection and reduction of a modeled bursting neuron, J. Comput. Neurosci. 3 (1996) 199–223.

[4] G.S. Cymbalyuk, R.L. Calabrese, Oscillatory behaviors in pharmacologically isolated heart interneurons from the medicinal leech, Neurocomputing 32–33 (2000) 97–104.

[5] J.G. Dilmore, B.S. Gutkin, G.B. Ermentrout, Effects of dopaminergic modulation of persistent sodium currents on the excitability of prefrontal cortical neurons: a computational study, Neurocomputing 26–27 (1999) 107–115.

[6] I.A. Fleidervish, A. Friedman, M.J. Gutnick, Slow inactivation of Na^+ current and slow cumulative spike adaptation in mouse and guinea-pig neocortical neurones in slices, J. Physiol. 493 (1) (1996) 83–97.

[7] A. Hill, J. Lu, M. Masino, Ø. H. Olsen, R. L. Calabrese, A model segmental oscillator of the leech heartbeat neuronal network, in preparation.
[8] F.C. Hoppensteadt, E.M. Izhikevich, Weakly Connected Neural Networks, Springer, New York, 1997.
[9] A.I. Khibnik, Yu.A. Kuznetsov, V.V. Levitin, E.V. Nikolaev, Continuation techniques and interactive software for bifurcation analysis of ODEs and iterated maps, Physica D 62 (1993) 360–367.
[10] V.I. Krinsky, Yu.M. Kokos, Analysis of the equations of excitable membranes: I. Reducing of Hodgkin–Huxley equations to the system of the second order, Biofizika 18 (1973) 506–511, in Russian.
[11] F. Nadim, Ø.H. Olsen, E. De Schutter, R.L. Calabrese, Modeling the leech heartbeat elemental oscillator: I. Interactions of intrinsic and synaptic currents, J. Comput. Neurosci. 2 (1995) 215–235.
[12] Ø.H. Olsen, F. Nadim, R.L. Calabrese, Modeling the leech heartbeat elemental oscillator: II. Exploring the parameter space, J. Comput. Neurosci. 2 (1995) 237–257.
[13] C.A. Opdyke, R.L. Calabrese, A persistent sodium current contributes to oscillatory activity in heart interneurons of the medicinal leech, J. Comput. Physiol. 175 (1994) 781–789.
[14] J. Rinzel, A formal classification of bursting mechanisms in excitable systems, in: E. Teramoto, M. Yamaguti (Eds.), Mathematical Topics in Population Biology, Morphogenesis and Neurosciences, Lecture Notes in Biomathematics, Vol. 71, Springer, Berlin, 1987, pp. 267–281.
[15] J. Rinzel, Y.S. Lee, Dissection of a model for neuronal parabolic bursting, J. Math. Biol. 25 (1987) 653–675.
[16] C.R. Yang, J.K. Seamans, Dopamine D1 receptor actions in layers V–VI rat prefrontal cortex neurons in vitro: modulation of dendritic-somatic signal interactions, J. Neurosci. 16 (1996) 1922–1935.

R.L. Calabrese

G.S. Cymbalyuk